

## Evaluation of the Interactions Between Hydrogen and Steel in Geothermal Conditions with H<sub>2</sub>S

Jean Kittel, François Ropital, François Grosjean, Gaurav Joshi

IFP Energies nouvelles, Rond-point de l'échangeur de Solaize, BP 3, 69360 Solaize, France

Jean.kittel@ifpen.fr

**Keywords:** Corrosion, hydrogen embrittlement, hydrogen permeation, HIC, SSC

### ABSTRACT

Geothermal fluids combine high temperature and high pressure conditions, leading to a severe risk of corrosion for the steel materials used in the well. Corrosivity is enhanced when acid gases such as CO<sub>2</sub> and H<sub>2</sub>S are present. In addition to localized or uniform corrosion, H<sub>2</sub>S also promotes hydrogen entry into the steels, resulting in a reduction of mechanical strength. Depending on the metallurgical properties of the steel and on the applied stresses, cracking may occur. Different types of H<sub>2</sub>S related cracking mechanisms have been identified, i.e. HIC (hydrogen induced cracking), or SSC (sulfide stress cracking), mainly based on the experience of oil and gas production where H<sub>2</sub>S is often present.

It is well recognized that 2 parameters govern the risks of hydrogen related failures, i.e. the instantaneous hydrogen flux at the metal surface related to the electrochemical reduction of proton associated with the corrosion reaction, and the cumulated amount of hydrogen dissolved in the metal. In order to examine these parameters, an original experimental device was used, allowing measuring hydrogen permeation in steel exposed to high-temperature / high-pressure environment. In parallel to the permeation measurements, HIC cracking experiments were performed. A good correlation was found between the extent of internal cracking and the hydrogen flux, for various experimental conditions in a pH range between 3.5 and 5.5, and H<sub>2</sub>S partial pressure between 0.01 bar and 1 bar.

### 1. INTRODUCTION

Recent evolution of the geothermal industry tends towards the development of medium entropy and high enthalpy resources. These resources are characterized by high temperatures (typically above 100 °C, and up to several hundreds of °C). Most of the time, the geothermal brine contains dissolved gases such as CO<sub>2</sub> and H<sub>2</sub>S. In aqueous solution, these gases act like weak acids (reactions 1 and 2), with pKa values of 6.4 for CO<sub>2</sub> and 7 for H<sub>2</sub>S at ambient temperature (J.P.Labbé 1979). Other corrosive species are also often present, such as chlorides, sulfates or ammonium. These brines may also contain high concentrations of dissolved minerals, like silicate, carbonate or sulfide. In addition, when CO<sub>2</sub> and H<sub>2</sub>S are re-injected into the well, which becomes a common practice, the temperature range between ambient and 100 °C may also be found. As a consequence, metals used in geothermal systems are subjected to a wide variety of corrosive environments and scaling issues. Scaling is mainly associated with temperature and pressure changes in the geothermal system, leading to modifications of solubilities of the dissolved minerals. Precipitates may also include metal cations issued from the corrosion of the equipment. Corrosion is often associated with acid solutions, either the brine itself, or condensates in contact with acid gases. The main electrochemical reactions thus correspond to iron oxidation (reaction 3), and proton reduction (reaction 4 or 5). Although proton reduction leads to the formation of “atomic hydrogen”, two radically different products may be formed by this reaction. Most of the time, two hydrogen atoms formed at the metal surface recombine into a di-hydrogen molecule, which dissolves into the aqueous solution until it reaches (quite rapidly) the solubility limit to form a gas bubble (reaction 4). However, hydrogen atom formed at the metal surface may also penetrate into the metal (reaction 5). This latter reaction is highly promoted by the presence of H<sub>2</sub>S, where it is quite common to observe that 50 % to 100 % of the cathodic hydrogen ends-up diffusing into the steel (Plennevaux et al. 2013; Deffo Ayagou et al. 2018).



Once absorbed into the metal, hydrogen is highly detrimental to the mechanical properties, resulting in the so-called hydrogen embrittlement (HE). Embrittlement may proceed by different mechanisms, depending on the metallurgical nature (cristallography, grain sizes, precipitates, inclusions...), mechanical aspects (residual or applied stresses, cyclic or static), temperature, etc.

In the case of low alloy steels, three cracking modes associated with the presence H<sub>2</sub>S are commonly considered.

SSC (sulfide stress cracking) is the first type of H<sub>2</sub>S cracking of low alloy steels. This cracking mode initiates at the metal surface and it required the combination of hydrogen entry and stresses. Cracked surface usually contains a brittle area oriented at 90° of the direction of the stresses. This type of cracks preferentially affects high-strength steels.

Hydrogen induced cracking (HIC) is associated with the interaction of hydrogen with internal defects such as inclusions, segregation bands. Hydrogen atoms may accumulate at the interface of such defects with the metal matrix, ultimately ending-up with decohesion

and cracks. Once internal voids are created into the metal, di-hydrogen molecules may form and induce high pressures, thus contributing to crack propagation. This type of cracks usually forms parallel to the rolling direction of the plates, and it affects mainly steel grades of medium strength (up to 700 MPa). Under the influence of stresses, either residual or applied, propagation may proceed in a stepwise manner, eventually resulting in the complete failure of the equipment (Crolet 2001). This type of cracking is called SOHIC (stress oriented HIC).

Since  $H_2S$  is often present in oil and gas reservoirs, most of published literature is associated with the petroleum industry since the discoveries of the Lacq field in France (15 %  $H_2S$  at a total pressure of 650 bar) or Jumping Pound in Canada (3 %  $H_2S$ ), which both stated their production in 1951. Lots of efforts driven by the petroleum industry and the steelmaking industry led to the development of sour resistant steel grades, together with the definition of quality control procedures for the selection of steels for use in  $H_2S$  environments. Guidelines provided by NACE International (NACE MR0175) and by the European Federation of Corrosion (EFC16 document) merged in 2001 as an ISO standard aimed at providing guidance for the selection of materials for use in  $H_2S$  containing environments in oil and gas production (NACE MR0175/ISO 15156). According to this document, the main parameters governing the risks of SSC are pH and  $H_2S$  partial pressure ( $P_{H_2S}$ ). These two parameters are used to define regions of environmental severity from region 0 (high pH, low  $P_{H_2S}$ ) where “no specific precautions are required for the selection of steels”, to region 3 (low pH, high  $P_{H_2S}$ ) where testing in severe conditions (1 bar  $H_2S$  at low pH) is necessary to ensure appropriate SSC resistance of selected steels (Figure 1). A preliminary diagram was also proposed recently for HIC (Kittel et al. 2007, 2008), but it requires more extensive testing to be validated before being incorporated in standard documents.

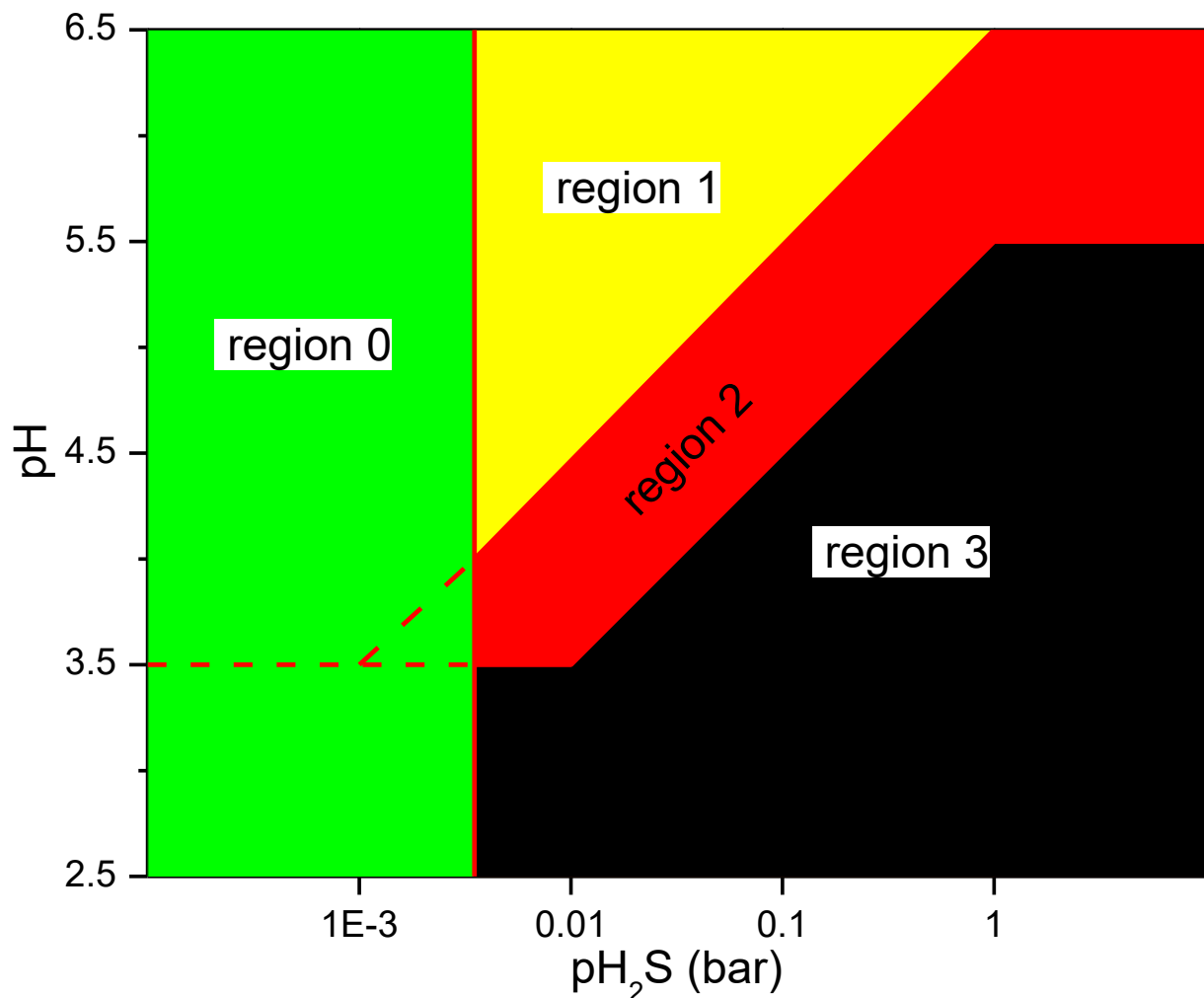


**Figure 1: SSC regions of environmental severity as per NACE MR0175 / ISO 15156-2.**

These types of cracking may also affect geothermal systems. For instance, several  $H_2S$  related failures of geothermal sites in Iceland were recently reported by Karlsdóttir et al. (Karlsdóttir 2012; Karlsdóttir et al. 2016; Karlsdóttir and Thorbjörnsson 2012). Geothermal industry of New Zealand has also reported several cases studies and recommendations for the selection of materials in  $H_2S$  rich geothermal brines (Lichti 2007; Lichti K 2017; Lichti K and Yanagisawa 2015). Even if geothermal brines do not contain liquid hydrocarbons, it is a common practice of geothermal industry to use the ISO recommendations for Oil and Gas production for material selection.

In this paper, we report a laboratory study on a low alloy steel with moderate resistance to  $H_2S$  cracking. This steel was tested in various environments, including some test conditions leading to internal cracking (HIC). In parallel, hydrogen permeation measurements with a hollow probe were performed, using the same steel exposed to the same environment as HIC samples. This type of hydrogen permeation probe is commonly used as a monitoring tool in refineries or oil & gas production lines, or for laboratory

studies (Crolet 2000). A similar device has also been used to study corrosion and hydrogen effects for geothermal applications (McAdam 1981). Comparisons were then made between the extent of cracking and hydrogen fluxes. Then, the hydrogen permeation methodology was applied in an autoclave, in order to evaluate the feasibility of measurements at high pressure and temperature.

## 2. EXPERIMENTAL METHODS

Two hydrogen permeation measurement techniques are commonly used in laboratory studies: the Devanathan-Stachurski electrochemical method (Devanathan and Stachurski 1964) for which the test sample is a flat steel membrane and the hollow sensor method (Crolet and Maisonneuve 2000) where the test sample is a steel cylinder with a small diameter hole drilled in the core (Figure 2). For both systems, steel specimens are exposed to the corrosive test solution, and hydrogen absorption is generated at the steel surface by the cathodic reaction (5). Then, absorbed hydrogen diffuses into the metal due to a concentration gradient, until it reaches the exit surface where it is extracted by the collecting method. For the Devanathan system, hydrogen extraction is ensured by the electrochemical oxidation of atomic hydrogen, i.e. reverse of reaction (5). The potentiostat measures the current density corresponding to this reaction, thus providing a direct measurement of the hydrogen diffusion flux. For the hollow sensor system, the exit surface of absorbed hydrogen corresponds to the walls of the internal cavity. As soon hydrogen has reached the sub-surface of the cavity, recombination into di-hydrogen molecule may occur, leading to a rise of pressure into the cavity (reaction 6). There, the hydrogen diffusion flux is obtained by the derivation of the curve representing the pressure evolution as a function of time.

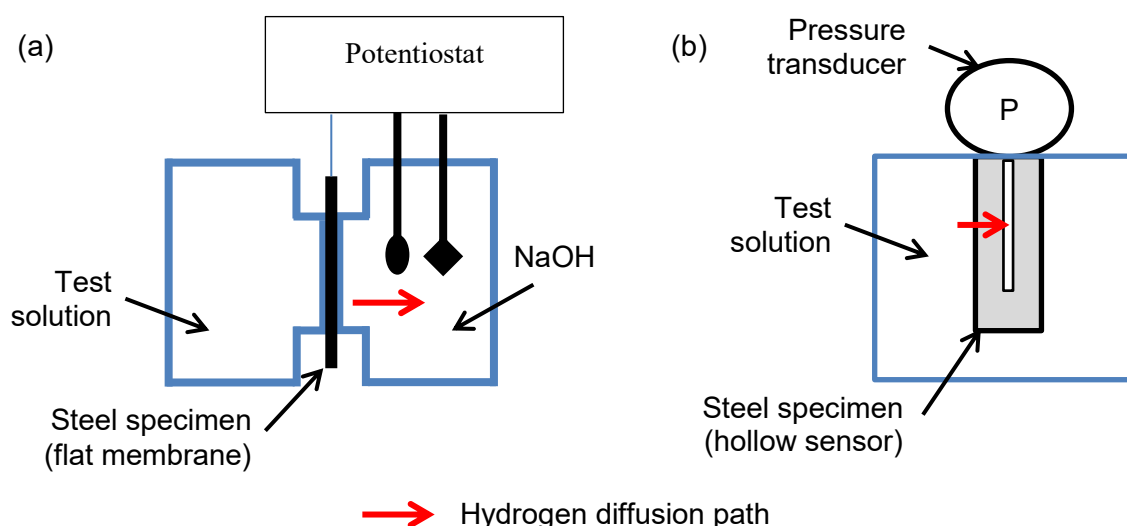


**Figure 2: Comparison of experimental methods for the measurement of hydrogen diffusion into steels exposed to corrosive and hydrogenating environment. (a) Devanathan-Stachurski electrochemical method ; (b) hollow sensor method.**

While the electrochemical method is the most widespread for hydrogen permeation studies related to  $H_2S$  environments, it is not easily adaptable to high pressure / high temperature environments. In this regard, the hollow sensor methodology appears to be much more versatile. It was thus chosen for this experimental work.

Most of the tests were performed in glass vessels at ambient pressure and temperature, with two types of specimens machined from a sweet service API X70 linepipe steel (see composition in Table 1): i/ a hollow sensor device for hydrogen permeation measurements and, ii/ 3 HIC specimens (100 mm long, 20 mm wide, and 14 mm thick) for cracking extent evaluation as per NACE TM0284-2016 and weight-loss corrosion rate measurements. Several tests were performed at various pH /  $P_{H_2S}$  conditions. Test durations were selected according to NACE TM0284-2016 recommendations, i.e. 4 days for  $H_2S$  partial pressure above 0.1 bar  $H_2S$ , 14 days for  $H_2S$  partial pressures between 0.01 bar and 0.1 bar, and 30 days for  $H_2S$  partial pressures between 0.003 bar and 0.01 bar. The detailed test matrix is given in Figure 3. For all the experiments, test solutions were composed of deionized water with 50 g/L NaCl and 4 g/L sodium acetate. pH was adjusted after saturation by acid gases by additions of de-aerated HCl or NaOH, depending on the target value. Test gases were either composed of pure  $H_2S$  (for the test conditions at  $P_{H_2S} = 1$  bar), or blends of  $H_2S$  and  $CO_2$  for the tests conditions at  $P_{H_2S}$  of 0.1 and 0.01 bar. The volume of the glass reactor was 2 L, resulting in a volume to surface ratio of 10 mL.cm<sup>-2</sup>.

**Table 1: Chemical composition (wt %) of the X70 steel used for the combined HIC / hydrogen permeation tests.**

C	Mn	Si	P	S	Cr	Ni	Mo	Cu	Nb	V
0.06	1.25	0.227	0.007	0.003	0.092	0.194	0.017	0.028	0.038	0.074

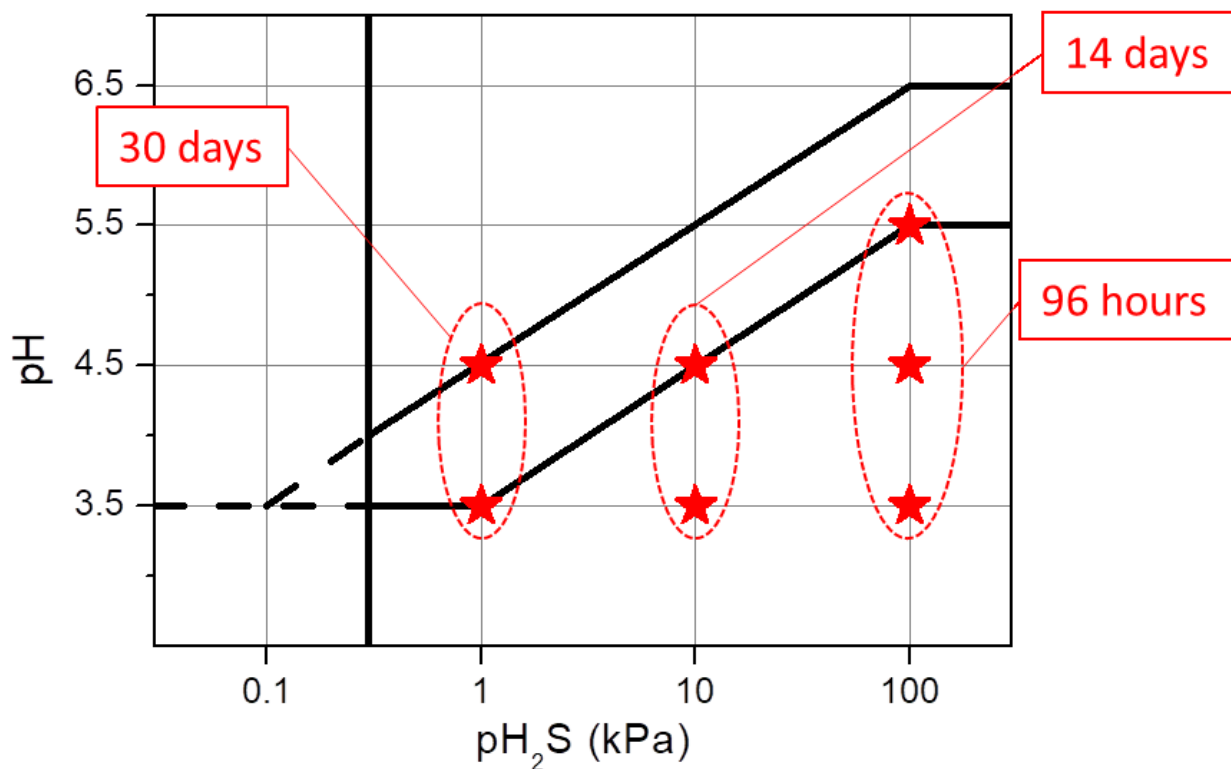


**Figure 3: test matrix for HIC exposures combined with hydrogen permeation measurements.**

In addition, another test was performed with hollow sensor devices inserted in an autoclave. The material used for the hollow sensor was pure iron capillary tubes, with 4 identical specimens used for repeatability evaluation. The test was carried out at a total pressure of 10 bar and at ambient temperature, but the pressure range of the equipment is 1 – 100 bar and it can operate up to 150°C. For this specific test, the test solution was composed of 35 g/L NaCl, with a bicarbonate buffer to reach a pH value of 4.5. The gas composition was 1% H<sub>2</sub>S + CO<sub>2</sub> leading to partial pressures of 0.1 bar for H<sub>2</sub>S and 9.9 bar for CO<sub>2</sub>.

### 3. RESULTS

#### 3.1. HIC Exposures at Various pH / P<sub>H<sub>2</sub>S</sub> and Hydrogen Permeation Measurements

After exposure in the test solutions, HIC steel samples were inspected by ultrasonic method to detect internal cracking. Ultrasonic inspection was applied with a 15 MHz transducer (1/4" diameter). For this type of steel (hot rolled plates), cracking often occurs at mid-thickness, in a plane parallel to the rolling direction. X-Y mapping of the specimen allowed mapping internal defects (C-Scan mode), from which a crack area ratio (CAR) was calculated as the ratio between the area of the defects and the total area of the specimen. Typical C-scans of ultrasonic inspections are presented on Figure 4.

As expected, HIC severity decreases at lower P<sub>H<sub>2</sub>S</sub> and at less acidic pH. It can be noted also that due to metallurgical heterogeneities, the scattering between CAR values of the specimens exposed to the same test environment can be quite high, which justifies the need to use at least 3 samples for this kind of tests. Corrosion rates are also greatly influenced by pH and P<sub>H<sub>2</sub>S</sub>. It seems however that the impact of pH dominates compared to P<sub>H<sub>2</sub>S</sub>. The scattering between the 3 samples for each test condition is also much lower than that of CAR measurements.

During each of these tests, hollow specimens were also exposed to the test solutions for hydrogen permeation measurements. The evolution of internal pressure with exposure time is presented on Figure 5. Quite surprisingly, the rate of H<sub>2</sub> pressure increase is similar for the two tests at 1 bar H<sub>2</sub>S and pH 3.5 or pH 4.5. On the other hand, as pH is increased to 5.5 and 1 bar H<sub>2</sub>S, hydrogen permeation drops to minute levels (no change of internal pressure after 4 days exposure). This latter result is thought to be due to the rapid formation of a protective iron sulfide layer, since the solubility of FeS is drastically reduced as pH increases. This surface layer may inhibit the hydrogen entry process. It also offers some protection against corrosion, hence reducing the overall rate of the electrochemical reactions. A similar trend is observed for the tests at pH 3.5 and 4.5 at 0.1 bar H<sub>2</sub>S, for which the hydrogen pressure rises are similar. However, when P<sub>H<sub>2</sub>S</sub> is further decreased (0.01 bar), differences of hydrogen permeation rates are observed between pH 3.5 and pH 4.5. For these tests, the rise of hydrogen pressure remained linear throughout the exposure period for all tests. This suggests that the concentration gradient of absorbed hydrogen between the entry face and the exit face did not change much during the tests, and also that the kinetic of hydrogen entry did not vary either. The slope of these curves thus corresponds to the steady-state hydrogen flux crossing the steel, as a result of electrochemical reactions at the external surface. Figure 6 presents the evolution of these slopes as a function of P<sub>H<sub>2</sub>S</sub>. Average values of CAR are also plotted for comparison. This last graph illustrates that a correlation seems to exist between the cracking extent and the hydrogen permeation flux. It is confirmed by the plot of CAR versus H-flux on Figure 7.

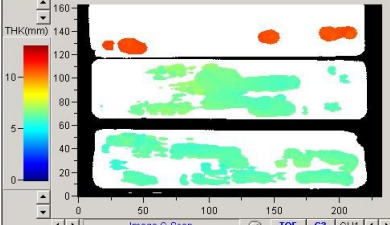
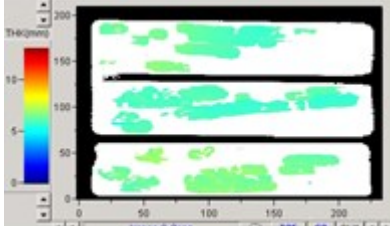
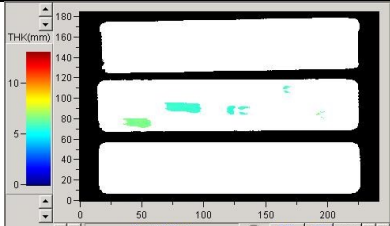
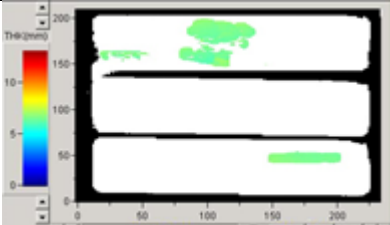
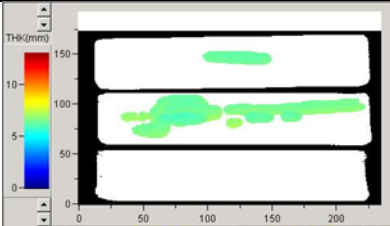
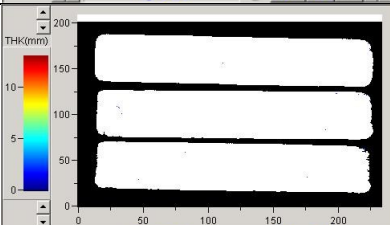
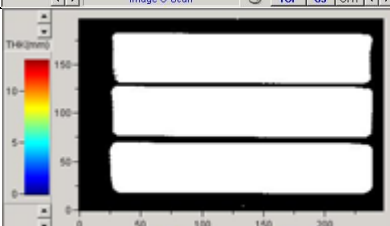
<p>pH 3.5 1 bar H<sub>2</sub>S</p>		<p>CAR = 9 % CAR = 36 % CAR = 41 %</p>	<p>Corrosion rate = 707 μm/year CR = 737 μm/year CR = 751 μm/year</p>
<p>pH 4.5 1 bar H<sub>2</sub>S</p>		<p>CAR = 29 % CAR = 39 % CAR = 32 %</p>	<p>CR = 532 μm/year CR = 547 μm/year CR = 554 μm/year</p>
<p>pH 5.5 1 bar H<sub>2</sub>S</p>		<p>CAR = 0 % CAR = 5 % CAR = 0 %</p>	<p>CR = 192 μm/year CR = 181 μm/year CR = 193 μm/year</p>
<p>pH 3.5 0.1 bar H<sub>2</sub>S</p>		<p>CAR = 18 % CAR = 0 % CAR = 6 %</p>	<p>CR = 498 μm/year CR = 497 μm/year CR = 535 μm/year</p>
<p>pH 4.5 0.1 bar H<sub>2</sub>S</p>		<p>CAR = 7 % CAR = 38 % CAR = 0 %</p>	<p>CR = 242 μm/year CR = 246 μm/year CR = 241 μm/year</p>
<p>pH 3.5 0.01 bar H<sub>2</sub>S</p>		<p>CAR = 0 % CAR = 0 % CAR = 0 %</p>	<p>CR = 579 μm/year CR = 601 μm/year CR = 589 μm/year</p>
<p>pH 4.5 0.01 bar H<sub>2</sub>S</p>		<p>CAR = 0 % CAR = 0 % CAR = 0 %</p>	<p>CR = 151 μm/year CR = 153 μm/year CR = 152 μm/year</p>

Figure 4: C-Scans and weight-loss corrosion rates of HIC specimens after exposure at various pH and P<sub>H<sub>2</sub>S</sub>.

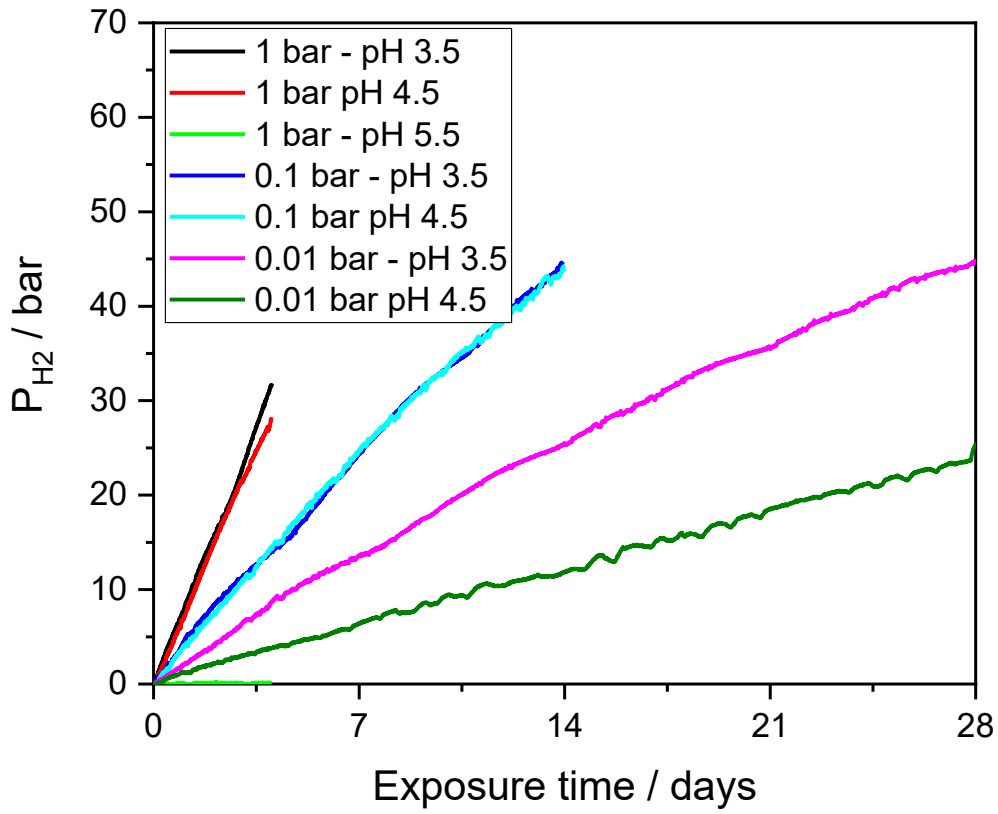


Figure 5: Time evolution of hydrogen pressure in the cavity of X70 hollow sensors exposed to aqueous test solutions at various pH and PH<sub>2</sub>S.

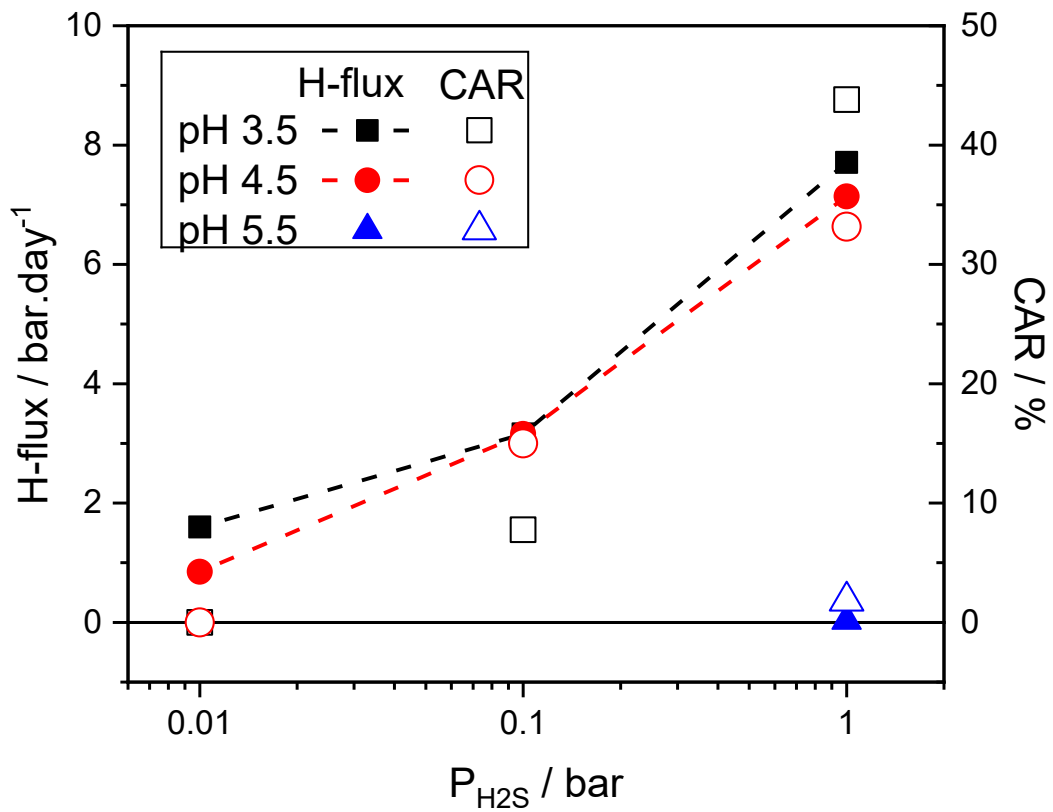


Figure 6: Evolution of hydrogen fluxes and CAR with PH<sub>2</sub>S.

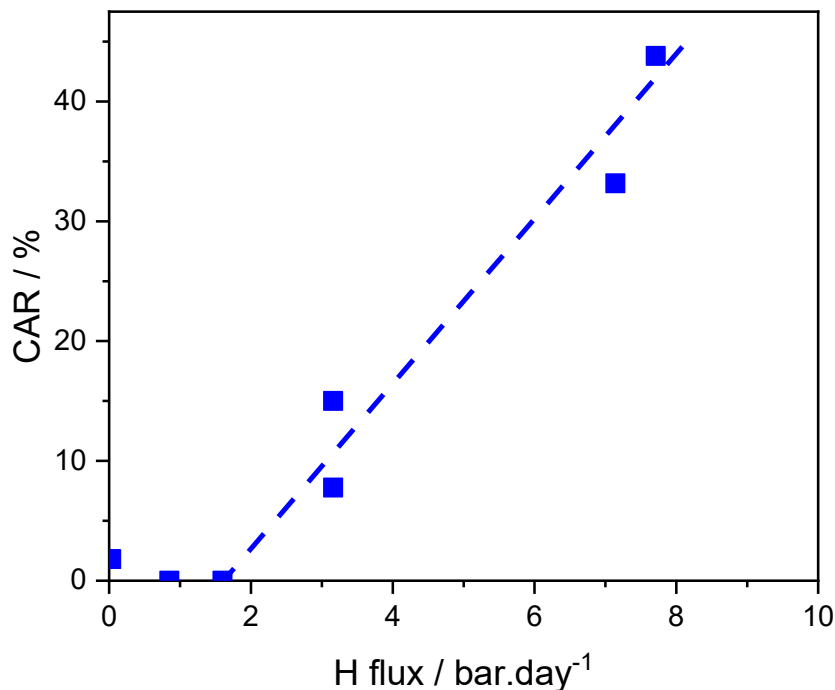


Figure 7: Correlation between CAR and hydrogen diffusion flux.

### 3.2 Hydrogen Permeation Measurements at Elevated Pressure

The rises of hydrogen pressure inside the cavities of four identical pure iron capillary tubes exposed to a test solution of pH 4.5 with 9.9 bar CO<sub>2</sub> and 0.1 bar H<sub>2</sub>S is presented on Figure 8. The pressure rise was similar for the four identical specimens with a dispersion band of approximately 10 %. For this test, the initial rate of pressure rise was close to 1 bar.day<sup>-1</sup>. This rate cannot be directly compared with previous results obtained on the X70 steel grade, since the geometry of the hollow sensors was not the same. Indeed, the pressure rise depends on the exposed surface of metal for hydrogen entry, and also on the volume of the internal cavity. It seems however that the pressure rise was in the same range as that previously observed at pH 4.5 and 0.1 bar H<sub>2</sub>S. For this test, we also observed a decrease of the slope of pressure rise with time, after 4 to 5 days. We interpret this change by the precipitation of corrosion products at the metal surface, leading to a decrease of the rate of electrochemical reactions, including proton reduction.

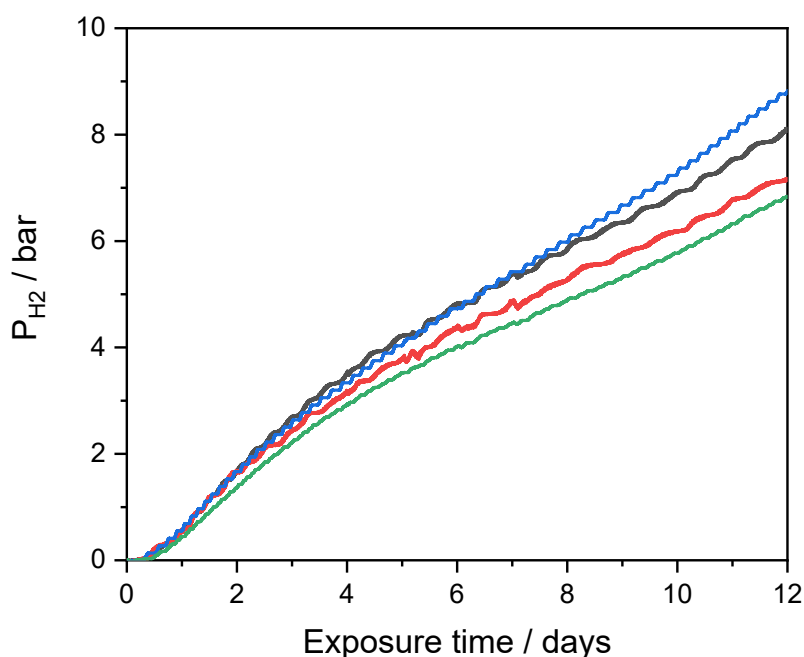


Figure 8: Time evolution of hydrogen pressure in the cavity of pure iron hollow sensors exposed to a test solution of pH 4.5, with 9.9 bar CO<sub>2</sub> and 0.1 bar H<sub>2</sub>S.

## CONCLUSION

The chemical composition of geothermal fluids often makes them highly corrosive. For low alloy steels, hydrogen embrittlement is associated with the production of “atomic hydrogen” by the cathodic reaction (reduction of  $H^+$ ). In presence of  $H_2S$ , the majority of the cathodic hydrogen penetrates into the steel, where it can diffuse and interact with metallurgical defects, hence affecting its mechanical properties. In order to evaluate the severity of the environment towards this type of problem, we used hydrogen permeation measurements with hollow sensors. Comparisons were made between hydrogen fluxes and the extent of internal cracking, determined after HIC exposures at various pH and  $P_{H_2S}$  according to the NACE TM 2084-2016 methodology. HIC specimens and hydrogen hollow sensors were made of the same API X70 linepipe steel. A good correlation was found between the extent of cracking and the hydrogen charging flux, illustrating the interest of this technique to predict the risks of  $H_2S$  cracking.

Then, the same methodology of hydrogen permeation was applied in an autoclave, in order to illustrate its relevance and ease of use at higher pressure and/or temperature. An experiment was conducted at a total pressure of 10 bar, with 4 identical sensors. The scattering between various sensors stayed below 10 %, which is quite satisfactory.

The tests presented in this paper were all obtained at ambient temperature and moderate pressure. As such, they are only representative of above ground equipment of the geothermal plant, after the heat exchangers or separator (e.g. condensers, re-injection lines, etc). However, this experimental technique can easily be implemented at much higher pressure and/or temperature, for the study of corrosive conditions in the well. In addition, while commercial monitoring devices based on hollow sensor measurements already exist, they usually use generic types of steel. The specific design of hollow sensors used in this work can easily be machined from steel plates of pipe sections, representative of the industrial equipment.

## ACKNOWLEDGEMENTS

The authors kindly thank Alexandre Bonneau for the implementation of the experimental setup. Thomas Pejot is also warmly acknowledged for his active participation in the HIC experiments.

## REFERENCES

- Crolet, J. L.: Relationships between stepwise cracking and SOHIC. Proceedings, Eurocorr 2001, Riva del Garda, Italy, 30 September - 4 October. The European Federation of Corrosion (2001).
- Crolet, J. L.; Maisonneuve, G.: Construction of a universal scale of severity for hydrogen cracking. Proceedings, Corrosion 2000 Paper 127. Orlando, FL (USA), 26-31 March. NACE International (2000).
- Deffo Ayagou, M.D. et al. : Corrosion, 74 (2018), 1192–1202.
- Devanathan, M. A. V. and Stachurski, Z.: Journal of the Electrochemical Society, 111 (1964) 619–623.
- ISO 15156-2:2015 Petroleum and Natural gas industries - Materials for use in  $H_2S$ -containing environments in oil and gas production - Part 2: Cracking resistant carbon and low alloy steels, and the use of cast iron.
- Karlsdóttir, S. N.: Corrosion, scaling and material selection in geothermal power production. In: Comprehensive Renewable Energy, vol. 7 – Geothermal Energy, T.I. Sigfusson Editor, (2012) 241–259.
- Karlsdóttir, S. N.; Hjaltason, S. M.; Ragnarsdóttir, K. R.: Corrosion testing in  $H_2S$  abatement system at hellisheidi geothermal power plant in Iceland. Proceedings, Corrosion 2016 Paper 7568. Vancouver, 07-10 March. NACE International (2016).
- Karlsdóttir, S. N. and Thorbjörnsson, I. O.: Hydrogen embrittlement and corrosion in high temperature geothermal well. Corrosion 2012 Paper 1467. Salt Lake City, UT (USA), 11-15 March. NACE International (2012).
- Kittel, J.; Martin, J. W.; Cassagne, T.; Bosch, C.: Hydrogen induced cracking (HIC) assessment of low alloy steel linepipe for sour service application - Laboratory testing. Proceedings, Eurocorr 2007. Freiburg, Germany, 9-13 September. The European Federation of Corrosion (2007).
- Kittel, J.; Martin, J. W.; Cassagne, T.; Bosch, C.: Hydrogen induced cracking (HIC) - Laboratory testing assessment of low alloy steel linepipe. Proceedings, Corrosion 2008. New-Orleans, LO (USA), 16-20 March. NACE International (2008).
- Labbé, J.P.: Matériaux & Techniques, 12 (1979) 423-428.
- Lichti K: Materials Selection Challenges for Geothermal Energy Projects. Proceedings, Corrosion 2017 paper 9258. New-Orleans, LA (USA), 26-30 March. NACE International (2017).
- Lichti K; Yanagisawa, N.: Geothermal energy and process issues. Proceedings, World Geothermal Congress 2015 Melbourne Australia (2015).
- Lichti, K. A.: Materials at High Temperatures, 24 (2007) 351–363.
- McAdam, G.D. et al. : Geothermics, 10 (1981) 115-131.
- Plennevaux, C. et al.: Electrochemistry Communications, 26 (2013) 17–20.